

Hydrogen-Bonding Interactions in Selected Super-molecular Systems: Electron Density Point of View

Tapan K. Ghanty* and Swapan K. Ghosh*

Theoretical Chemistry Section, RC & CD Division, Chemistry Group, Bhabha Atomic Research Centre, Mumbai 400 085, India

Received: May 5, 2003; In Final Form: June 19, 2003

Ab initio and density functional theoretical calculations have been performed to quantify the hydrogen-bonding interactions for selected supermolecular systems, experimental investigations on which have been reported very recently (*Angew. Chem., Int. Ed.* **2001**, *40*, 3240). An analysis and rationalization of the nature of pairwise interactions in different hydrogen bonds involved in these ternary supermolecular systems is presented that uses the frameworks of Morokuma energy decomposition as well as Bader's topological theory of atoms in molecules involving the electron density $\rho(\mathbf{r})$, its Laplacian $\nabla^2\rho(\mathbf{r})$, and also other related quantities at the bond critical points. The pK_a values of the aromatic acids, which have been used earlier to rationalize the specific intermolecular interactions between aromatic acids (hydrogen-bond donor) and isonicotinamide (hydrogen-bond acceptor as well as donor), are, however, found not to show any regular trend with the calculated binary interaction energy values or the electron density-based bonding parameters using experimental geometries. The calculated quantities corresponding to the computationally optimized geometries of the molecular species, however, do show some regular trends with the corresponding pK_a parameters.

1. Introduction

Among the weak intermolecular interactions, hydrogen bonding has been the subject of increasing research activities^{1–5} in recent years due to its importance in many chemical and biological systems and processes. The essence of the physical interactions that contribute to hydrogen bonding has been the subject of numerous discussions in the literature, and even the nature of interactions involved in an O–H···O hydrogen bond sometimes appears to be controversial.^{6,7} While the key feature in inorganic supramolecular systems⁸ is mostly the metal-ion coordination, it is the hydrogen bonding that plays^{9,10} an important role for assembling^{11–13} organic molecules through crystal engineering or for stabilizing supramolecular aggregates in water. Although the procedures for synthesizing covalently bonded molecular species with desired structures and properties have more or less been standardized, in contrast, the supramolecular synthesis involving noncovalent interactions such as hydrogen bonding (through crystal engineering) has yet to attain the same level of sophistication. Higher levels of refinement and versatility in crystal engineering require identification of reliable supramolecular synthons¹⁴ and synthetic strategies for building desired multicomponent structures. In recent years, many systematic studies have been reported demonstrating the synthesis of molecular assemblies with increasing complexity and dimensionality. Studies involving ternary supermolecules reporting^{15,16} 1:1:1 ternary cocrystal-containing supermolecules, which consist of three different components, have been rather recent. The recently reported synthetic strategy of Aakeröy et al.¹⁵ has been based on the rule of thumb that in a system with various hydrogen-bonding functionalities “the best hydrogen-bond donor and the best hydrogen-bond acceptor will preferentially form hydrogen bonds to one another” and the second-

best donor will form a hydrogen bond to the second-best acceptor and so on. It has also been assumed that a small number of specific intermolecular interactions can provide a large part of the stabilization energy of molecular crystals. For this purpose, different derivatives of benzoic acids (H-bond donor) and isonicotinamide (H-bond acceptor) molecules have been considered and an attempt has been made to rationalize the nature of specific intermolecular interactions intuitively by using the pK_a values of the constituent carboxylic acids. Although it is sometimes possible to qualitatively follow the synthetic strategies to construct supermolecular systems by considering the possible interactions judged intuitively through the parameters obtained from conventional chemical concepts such as pK_a values, as considered recently, an alternative elegant way to do this would be to quantify^{17–19} the intermolecular interactions by use of ab initio theoretical techniques for a set of binary or ternary systems. Although the intermolecular interaction energy provides the gross features about the nature and quantification of an interaction, more precise and detailed qualitative and quantitative information and insight can be retrieved through consideration of other aspects of the electron density distribution.

One such tool that has been quite valuable in providing insight into various aspects of the structure and bonding in molecules involves the topological analysis²⁰ of the electron density $\rho(\mathbf{r})$, which has proved to be highly successful. Recently this approach has been extensively used^{21–26} for the studies of interesting and unusual bonding aspects in several molecular systems including $(H_2O)_2^+$ and $(H_2S)_2^+$. The interactions underlying the design strategy of supermolecules can be rationalized through detailed studies of the topological aspects of their electron distribution. We thus propose to employ the topological theory of atoms in molecules (AIM),²⁰ which has been known to provide a rigorous procedure to partition a molecular system into its atomic fragments defined by the gradient vector field $\nabla\rho(\mathbf{r})$ and discuss chemical bonding through the bond path and bond critical point

* Corresponding authors: e-mail: skghosh@magnum.barc.ernet.in and tapang@apsara.barc.ernet.in.

properties. The AIM framework builds a bridge between the quantitative results obtained from quantum chemical calculations or experiments and the traditional chemical concepts. The study presented here is thus intended not only to investigate the total interaction energy of the different systems but also to provide a rationalization through an analysis of the electron density distribution for different bonding situations present in the ternary supermolecules as well as the Morokuma energy decomposition,²⁷ which partitions the total interaction energy into its different components such as electrostatic, polarization, charge transfer, and exchange repulsion and is often used by chemists for understanding the intermolecular interactions.^{7,27,28}

The plan of the paper is as follows. We discuss the computational method in section 2 and the results of numerical calculations in section 3. Finally, we present the concluding remarks in section 4.

2. Computational Methods

Ab initio molecular orbital methods have been used to investigate the electronic structures of the supermolecular systems considered here. Experimental geometries have been used for the calculation of the intermolecular interaction energies as well as bonding analysis that uses the calculated electron density distributions. For computational economy, only the pairwise interactions have been considered, as the third component would have negligible effect on the calculated results for intermolecular interactions between the first and second components. Density functional theory- (DFT-) based calculations have been performed with the B3LYP²⁹ exchange-correlation energy density functional (three-parameter Becke exchange and Lee–Yang–Parr correlation) and 6-31G(d,p) basis set. Starting with the experimental geometries as initial guess, geometries have also been optimized at the same level of theory. In the preparation of the cocrystal as reported in the original paper, the first step involved the mixing of equimolar amounts of a weaker acid, a stronger acid, and isonicotinamide to react in an aqueous solution. The initial stage of formation of supermolecules thus involved the solution-phase environment. It would therefore be interesting to study the effect of solvent on the intermolecular interactions, which has been taken into account here by using the polarizable continuum model (PCM).³⁰ The ab initio calculations in this work have been performed with the GAMESS³¹ electronic structure program. The topological properties of the electronic charge density have been calculated with the program AIMPAC.³²

3. Results and Discussion

The three ternary systems (I–III) of interest, which differ only in the third component, are shown in Figure 1. Ab initio calculations have been performed on the dimers of the first and second components as well as the second and third components by using the available experimental geometry and also the optimized geometries. The interaction energies are obtained by subtracting the energies of the corresponding monomers calculated at the same level of ab initio procedure. The calculated interaction energies ΔE_{12} (between components 1 and 2) and ΔE_{23} (between components 2 and 3) for all three systems are reported in Table 1. The values of ΔE_{12} corresponding to the optimized geometry are thus clearly identical for all three systems, while the value of ΔE_{23} also differ very little in the three cases in gas phase as well as in the presence of the solvent, although the third component is different.

Also included in Table 1 are the pK_a values of components 1 and 3. The pK_a value characteristic of component 1 (which is

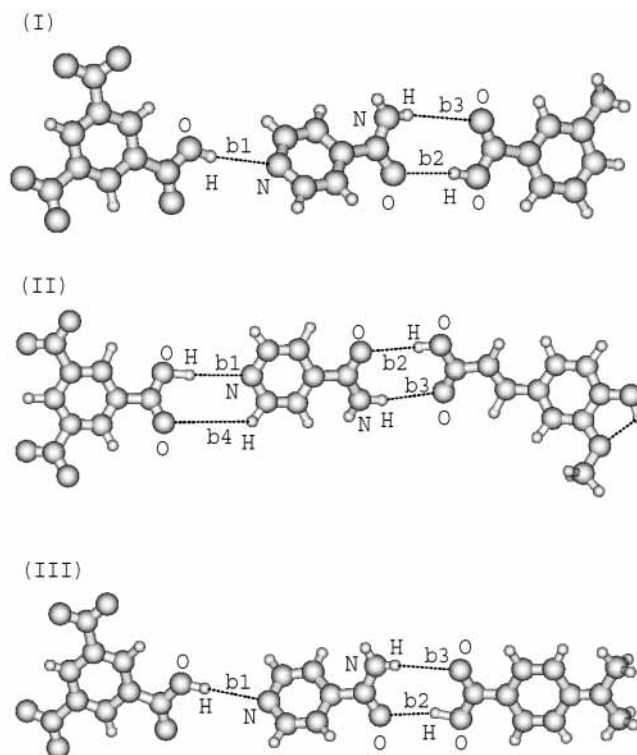


Figure 1. Structures of the three ternary supermolecules considered in this work: system **I**, 1:1:1 complex of 3,5-dinitrobenzoic acid, isonicotinamide, and 3-methylbenzoic acid; system **II**, 1:1:1 complex of 3,5-dinitrobenzoic acid, isonicotinamide, and 4-hydroxy-3-methoxycinnamic acid; system **III**, 1:1:1 complex of 3,5-dinitrobenzoic acid, isonicotinamide, and 4-(dimethylamino)benzoic acid.

the same in all three systems) alone obviously cannot be sufficient to rationalize the differences of ΔE_{12} values (calculated from experimental geometries) in the three cases. The interaction energies ΔE_{23} (with different third components), although they are different for the three cases (systems I–III), cannot again be rationalized on the basis of the pK_a values of the third component alone. In fact, the interaction energy ΔE_{23} is found to be higher for system **III**, where the pK_a value is also high, which is counterintuitive. It is to be noted that although the Hartree–Fock calculated interaction energies differ in magnitude from the corresponding density functional results, the trend remains the same. Thus, it is clear that the use of pK_a is not sufficient for supermolecule design strategy. On the other hand, ab initio electronic structure calculations of pairwise dimers provide more detailed information about the nature of interaction and hence are expected to play a key role in the design strategy.

It is to be noted that the interaction energies for system **II** calculated at the B3LYP level for the optimized geometry and the experimental geometry are respectively -13.7 and -30.0 kcal/mol. This difference in energy is extremely large and may be due to the fact that, for the experimental case, the monomer geometries are taken as the monomer-in-complex. In view of this difference, we have calculated the deformation energy of the monomers (the energy needed to deform the monomers from their optimal structure to the structure in the complex) and the results are reported in Table 2. It is observed that the deformation energies vary from 12.5 to 97.1 kcal/mol for different monomers, indicating that the monomer geometry in the complex (experimental structure) corresponds to higher energy than that of the optimized structure for all the monomers. Thus, it is clear that the optimized structures are really the structures of minimum energy. If these deformation energy values are

TABLE 1: Calculated Interaction Energies^a by Hartree–Fock and Density Functional Theory with B3LYP Functional

system	$pK_a(1)^b$	ΔE_{12}^c	ΔE_{12}^d	ΔE_{12}^e	ΔE_{12}^f	$pK_a(3)^g$	ΔE_{23}^c	ΔE_{23}^d	ΔE_{23}^e	ΔE_{23}^f
I	2.8	−13.7	−10.3	−8.5	−12.3	4.3	−18.9	−13.3	−14.5	−17.9
II	2.8	−13.7	−10.3	−26.3	−30.0	4.4	−18.7	−13.0	−15.5	−21.8
III	2.8	−13.7	−10.3	−14.2	−18.4	6.5	−18.5	−13.0	−18.6	−17.7

^a Energies are given in kilocalories per mole. ^b pK_a values for the first component. ^c Calculated with optimized geometry and B3LYP method. ^d Calculated with optimized geometry in the presence of solvent and B3LYP method. ^e Calculated with experimental geometry and Hartree–Fock method. ^f Calculated with experimental geometry and B3LYP method. ^g pK_a values for the third component.

TABLE 2: Deformation Energy^a Values for the Monomers and Complexes Calculated by Hartree–Fock and Density Functional Theory

system	method	DE_1^b	DE_2^c	DE_3^d	DE_{12}^e	DE_{23}^f	$DE_{12} - DE_1 - DE_2$	$DE_{23} - DE_2 - DE_3$
I	HF ^g	6.1	59.5	52.2	65.8	110.3	0.2	−1.5
	DFT ^h	15.1	68.6	58.3	84.6	127.4	0.9	0.6
II	HF ^g	30.3	9.6	38.2	22.2	28.4	−17.7	−19.4
	DFT ^h	26.3	12.5	19.2	19.8	30.1	−19.0	−1.7
III	HF ^g	29.9	49.1	92.5	73.5	136.0	−5.5	−5.6
	DFT ^h	35.6	56.8	97.1	86.8	149.7	−5.6	−4.1

^a Deformation energy is defined as the energy needed to deform the optimized structure to the corresponding experimental geometry. Energies are given in kilocalories per mole. ^b Deformation energy of monomer 1. ^c Deformation energy of monomer 2. ^d Deformation energy of monomer 3. ^e Deformation energy of the dimer consisting of monomers 1 and 2. ^f Deformation energy of the dimer consisting of monomers 2 and 3. ^g Calculated with HF optimized geometry and HF method. ^h Calculated with B3LYP optimized geometry and B3LYP method.

TABLE 3: Morokuma Analysis^a of Interaction Energies^b Using Optimized Geometries

system	interaction	method	ES	EX	PL	CT	MIX	ΔE	BSSE ^c
I/II/III	1–2	HF ^d	−17.9	13.3	−3.9	−4.5	0.5	−12.4	1.4
		DFT ^e	−21.2	20.5	−5.4	−6.7	1.4	−11.3	1.0
I	2–3	HF ^d	−21.0	14.3	−3.3	−4.8	−0.8	−15.6	2.0
		DFT ^e	−29.5	26.7	−5.6	−8.2	−1.2	−17.7	2.2
II	2–3	HF ^d	−20.5	13.9	−3.2	−4.7	−0.9	−15.3	2.1
		DFT ^e	−29.1	26.4	−5.3	−7.9	−1.3	−17.2	2.3
III	2–3	HF ^d	−20.8	14.1	−3.2	−4.7	−0.9	−15.5	2.1
		DFT ^e	−29.3	26.4	−5.4	−8.0	−1.2	−17.4	2.2

^a For explanation of different terms see text. ^b Calculated by the HF/6-31G(d,p) method. Energies are given in kilocalories per mole. ^c Basis-set superposition error. ^d Calculated with HF/6-31G(d,p) optimized geometries. ^e Calculated with B3LYP/6-31G(d,p) optimized geometries.

added to the calculated pair interaction energies from experimental geometries, the resulting interactions become apparently repulsive. Thus, it is the crystal packing forces that provide the necessary energetic compensation for the formation of the stable solid-state assembly. The deformation energy values also might be quite inaccurate due to considerable uncertainty in the experimental geometry from X-ray-based methods.

Further insight is provided by a Morokuma partitioning of the interaction energy in terms of an electrostatic (ES), polarization (PL), exchange–repulsion (EX), and charge transfer (CT) components including other higher order terms (MIX). The ES term representing the total Coulombic interaction between the free monomer charge distributions includes the interactions of all permanent charges and multipoles and may be either attractive or repulsive. The PL term, which is always attractive, denotes the polarization interaction, i.e., the effect of the distortion of the electron distribution of monomer 1 by monomer 2 and vice versa and includes the interactions between all permanent charges or multipoles and induced multipoles. The origin of EX is the interaction caused by the exchange of electrons between the monomers satisfying the Pauli principle and this contribution accounts for the short-range repulsion due to overlap of electron distribution of one monomer with that of another monomer. CT is caused by the electron delocalization interaction, i.e., the interaction caused by charge transfer from the occupied molecular orbitals of monomer 1 to the vacant molecular orbitals of monomer 2 and vice versa. The MIX term is the difference between the total interaction energy and the sum of the above four components and accounts for higher order interactions.

In view of the large difference between the calculated interaction energies obtained from the experimental and optimized geometries and also the unreliability of the position of a hydrogen atom in an H-bond as obtained through X-ray methods, we report here the results of Morokuma analysis of the interaction energy based on the optimized geometries (both Hartree–Fock and density functional B3LYP) only. From the calculated values of all these quantities reported in Table 3, it is clear that the ES and EX contributions are of the same order but with opposite sign, thus almost canceling each other, and it is the PL and CT contributions that play the dominating role in predicting the variations of the overall interaction energies. However, the ES and EX contributions obtained with DFT optimized geometries are found to be closer than those of the corresponding results with HF geometries. It is also evident that the interaction energies ΔE_{12} and ΔE_{23} , denoting the stronger and weaker contributions, respectively, show some regular features in the energy components. The 1–2 interaction ΔE_{12} is the same for all the three systems, while the 2–3 interaction ΔE_{23} is minimum for system **II**. The same is true for the ES and EX components as well. It is also clear that the relative interaction energy values remain almost unchanged even after inclusion of the basis-set superposition error. It is to be noted that the relative total interaction energy value remains almost the same irrespective of the calculation method used for geometry optimizations and the absolute energy difference ranges from 1.1 to 2.1 kcal/mol.

Apart from the interaction energies, a more intuitive appeal comes from consideration of the electron density-based topological parameters, such as the values of the electron density

TABLE 4: Topological Analysis of the Bond Length (R), Bond Order (BO), Electron Density [$\rho(r)$], and the Laplacian of the Electron Density [$\nabla^2\rho(r)$]

property	system	optimized geometry ^a			experimental geometry		
		O–H···N (b1)	O···H–O (b2)	N–H···O (b3)	O–H···N (b1)	O···H–O (b2)	N–H···O (b3)
R (Å)	I	1.703 (1.703)	1.641 (1.641)	1.844 (1.844)	1.669	1.635	2.115
	II	1.703 (1.703)	1.674 (1.674)	1.806 (1.806)	1.366	1.658	1.827
	III	1.703 (1.703)	1.651 (1.651)	1.844 (1.844)	1.500	1.520	1.975
BO	I	0.166 (0.181)	0.168 (0.175)	0.136 (0.128)	0.161	0.158	0.106
	II	0.166 (0.181)	0.162 (0.170)	0.145 (0.137)	0.290	0.160	0.138
	III	0.166 (0.181)	0.164 (0.173)	0.143 (0.135)	0.215	0.200	0.139
$\rho(r)$ (eÅ ⁻³)	I	0.3577 (0.3610)	0.3435 (0.3462)	0.2193 (0.2193)	0.3826	0.3475	0.1269
	II	0.3577 (0.3610)	0.3172 (0.3199)	0.2389 (0.2389)	0.8624	0.3293	0.2289
	III	0.3577 (0.3610)	0.3361 (0.3394)	0.2213 (0.2213)	0.5824	0.4785	0.1701
$\nabla^2\rho(r)$ (eÅ ⁻⁵)	I	2.6388 (2.5665)	3.4220 (3.3907)	2.2219 (2.2556)	3.1883	3.7763	1.3278
	II	2.6388 (2.5665)	3.1931 (3.1666)	2.4533 (2.4894)	-3.3955	3.4317	2.4123
	III	2.6388 (2.5665)	3.3955 (3.3642)	2.2026 (2.2364)	1.6411	0.8145	1.8725

^a Corresponding values in the presence of solvent are given in parentheses.

and its Laplacian at the bond critical point of the O–H···N or O···H–O weak bonds. We thus analyze the nature of interactions involved in the three ternary systems within the framework of Bader's topological theory of atoms in molecules (AIM). A bond critical point (point corresponding to $\nabla\rho = 0$ and normally abbreviated as BCP) is found between each pair of nuclei, which are considered to be linked by a chemical bond, with two negative curvatures (λ_1 and λ_2) and one positive curvature (λ_3), and is denoted as (3, -1) critical point. The bond ellipticity (ϵ) defined in terms of the two negative curvatures as $\epsilon = (\lambda_1/\lambda_2 - 1)$ reflects the deviation of the charge distribution of a bond path from axial symmetry, thus providing a sensitive measure of the susceptibility of a system to undergo a structural change. The Laplacian of the electronic charge density ($\nabla^2\rho$) indicates whether the electron density is locally concentrated ($\nabla^2\rho < 0$) or depleted ($\nabla^2\rho > 0$) and provides a detailed map of the basic and acidic regions of a molecule. A quantitative comparison of the nature of bonding should however follow from the values of this quantity at the BCP and also from the other BCP properties. Thus, a value of $\nabla^2\rho < 0$ at a BCP is unambiguously related to the covalent character of a bond, indicating a sharing of electrons and referred to as "shared"-type interaction, while $\nabla^2\rho > 0$ implies a "closed-shell"-type interaction as found in noble gas repulsive states, ionic bonds, hydrogen bonds, and van der Waals molecules. Bader has also defined a local electronic energy density as $E_d(r) = G(r) + V(r)$, where $G(r)$ and $V(r)$ correspond to local kinetic and potential energy densities, respectively. The sign of $E_d(r)$ determines whether accumulation of charge at a given point r is stabilizing [$E_d(r) < 0$] or destabilizing [$E_d(r) > 0$].

The calculated results of the topological indices corresponding to optimized geometries of the three systems reported in Table 4 reveal that, for a particular bond, the BCP electron density and Laplacian values are almost the same for all the three systems (I–III). Even the presence of solvent has negligible effect on these topological properties. From the calculated results

for the O–H···N (b1) interaction (in the case of 1–2 interactions) as well as for O···H–O (b2) and N–H···O (b3) interactions (in the case of 2–3 interactions), it is clear that the comparatively stronger bond b1 is associated with higher electron density at the BCP as well as higher bond order, as expected. In the case of 2–3 interactions, however, there are two weak bonds b2 and b3 (see Figure 1) and it is difficult to correlate the interaction energy with the BCP parameters for any one of them. A meaningful way to judge the relative strength of the two weak bonds in 2–3 interactions would be to follow the weighted average of the BCP electron density values. It is clear from the $\rho(b2)/[\rho(b2) + \rho(b3)]$ and $\rho(b3)/[\rho(b2) + \rho(b3)]$ values at BCP for the b2 and b3 bonds that the O···H–O bond plays a relatively more significant role in all the systems I–III. It is to be noted that additionally one C–H···O hydrogen bond is also present between the components 1 and 2 in the system II (denoted as b4 in Figure 1). It is reflected by the existence of a bond critical point in the corresponding C–H···O bond, which is otherwise absent for the corresponding bond in systems I and III. Discussions on various aspects of the C–H···O interaction have been reported^{33–36} recently.

For the sake of comparison, also included in Table 4 are the results corresponding to the experimental geometries. While the general conclusions remain almost the same, the presence of one strong O–H···N bond (with negative Laplacian value and shortest bond length) along with the existence of one C–H···O interaction account for the large value of the interaction energy (ΔE_{12}) between the components 1 and 2 in system II. The most significant difference between the optimized and experimental geometries is also reflected in the bond length of O–H···N hydrogen bonds, particularly in systems II and III, as evident from the geometrical parameters reported in Table 4. This may be attributed to the fact that the optimized geometry corresponds to only the isolated system while the experimental geometry incorporates contribution from crystal packing forces present in solid phase.

It would be interesting to further provide an in-depth analysis using the results from optimized geometries, which are free from unknown experimental artifacts. Here the results have been found to be perfectly clear, viz., the 1–2 interaction is always weaker than the corresponding 2–3 interaction in both the sets of results obtained either from HF or DFT geometries (Tables 1 and 3). Apparently it seems that there is no regular trend between the calculated interaction energy values with pK_a parameters. However, it is to be noted that each 2–3 interaction involves two H-bonds while the 1–2 interaction involves only one H-bond. Out of the two H-bonds in a particular 2–3 interaction, the O···H–O (b2) bond is likely to be of almost the same strength as that of the N–H···O (b3) bond (as reflected through the calculated BCP electron density and Laplacian quantities for the optimized geometry). Thus, considering half of the 2–3 interaction energy, one can observe that the 1–2 interaction is definitely stronger than the two others as expected from the pK_a values. It is still valid for the results obtained with experimental geometries; however, the drastic variation of ΔE_{12} for the three species having same components (and obviously the same pK_a value for the acid, component 1) cannot be rationalized by the same pK_a value alone, and perhaps the uncertainty in the experimental geometry might be responsible for these deviations. It is also important to note that the experimental geometries have been obtained for a solid sample, and our optimization level considers molecules/supramolecules in a vacuum. Thus, the experimental geometries might involve the effect of crystal packing forces in addition to the attractive intermolecular interactions through H-bonding, which might be another reason for the discrepancy between the two sets of results obtained from experimental and optimized geometries. It may be noted that the variations of ΔE_{23} corresponding to the optimized geometries among the three systems are too small to be rationalized with the pK_a values.

In this context, it should be noted that recently the uncertainty regarding the location of the H atom in O–H···O and N–H···O hydrogen bonds (obtained through X-ray diffraction experiments) has been well documented in the literature.^{16,37,38} Although neutron diffraction has been shown^{16,37,38} to be a better method for locating the position of the H atom in a H-bond (as compared to X-ray diffraction), it is also possible to find more or less the exact position of the H atom in hydrogen bonds by use of ab initio quantum chemical calculations through geometry optimizations without any symmetry constraint. In the present work, we have used Hartree–Fock as well as density functional theory to obtain the optimized geometries of the systems, and the difference in the H-bond lengths as obtained from the two sets of calculations are found to be rather small, suggesting consistency in the calculated values for the H-bond lengths. Thus, in the absence of any neutron diffraction studies in the systems considered in our work, the present geometries obtained by us through ab initio methods can be considered to be more accurate in comparison to the corresponding reported experimental geometries for the supermolecules.

4. Concluding Remarks

In summary, we have reported here ab initio calculation and a detailed analysis of the energetics of the pairwise hydrogen-bonding interaction in different ternary supermolecules through Morokuma energy decomposition. We have also investigated the various density-related quantities at the bond critical points and their role in rationalization of the nature of interactions. It is observed that the pK_a values of the aromatic acids, which have been used earlier to rationalize the specific intermolecular

interactions, do not show any regular trend with the calculated interaction energy values or the electron density-based bonding parameters obtained for experimental geometries. However, the calculated quantities corresponding to the computationally optimized geometries of the molecular species do show some trends with the corresponding pK_a parameters.

In this work, our objective has been to study the specific intermolecular interactions toward the design strategy for the construction of supermolecules from the isolated molecules. Real crystals are generally formed through the three-dimensional solid-state assembly of such supermolecules (building blocks), which involve crystal-packing forces in addition to the specific intermolecular interactions between two molecules in a vacuum (gas phase) or in solution. The aim has been to provide insight into the first step, viz., construction of supermolecules from isolated molecules considering the specific intermolecular interactions through interaction energy and electron density-based bonding parameters. The second step, which involves the three-dimensional assembly of the supermolecules in the solid state, has not been considered here.

Acknowledgment. It is a pleasure to thank Dr. T. Mukherjee and Dr. J. P. Mittal for their kind interest and encouragement.

References and Notes

- (1) Desiraju, G. R.; Steiner, T. *The Weak Hydrogen Bond: IUCr Monographs on Crystallography*; Oxford University Press: New York, 1999.
- (2) (a) Scheiner, S. *Annu. Rev. Phys. Chem.* **1994**, *45*, 23. (b) Scheiner, S. *Hydrogen Bonding: A Theoretical Perspective*; Oxford University Press: New York, 1997.
- (3) (a) Jeffrey, G. A.; Saenger, W. *Hydrogen Bonding in Biological Structures*; Springer: Berlin, 1991. (b) Jeffrey, G. A. *An Introduction to Hydrogen Bonding*; Oxford University Press: New York, 1997.
- (4) Gordon, M. S.; Jensen, J. H. *Acc. Chem. Res.* **1996**, *29*, 536.
- (5) Alkorta, I.; Rozas, I.; Elguero, J. *Chem. Soc. Rev.* **1998**, *27*, 163.
- (6) Isaacs, E. D.; Shukla, A.; Platzman, P. M.; Hamann, D. R.; Barbiellini, B.; Tulk, C. A. *Phys. Rev. Lett.* **1999**, *82*, 600.
- (7) Ghanty, T. K.; Staroverov, V. N.; Koren, P. R.; Davidson, E. R. *J. Am. Chem. Soc.* **2000**, *122*, 1210.
- (8) *Transition Metals in Supramolecular Chemistry*; Sauvage, J. P., Ed.; Wiley: Chichester, U.K., 1999.
- (9) Prins, L. J.; Reinhoudt, D. N.; Timmerman, P. *Angew. Chem., Int. Ed.* **2001**, *40*, 2382.
- (10) Steiner, T. *Angew. Chem., Int. Ed.* **2002**, *41*, 48.
- (11) Lehn, J. M. *Supramolecular Chemistry*; VCH: Weinheim, Germany, 1995.
- (12) Desiraju, G. R. *Crystal Engineering: The Design of Organic Solids*; Elsevier: Amsterdam, 1989.
- (13) *Perspectives in Supramolecular Chemistry: The Crystal as a Supramolecular Entity*, Vol. 2; Desiraju, G. R., Ed.; Wiley: Chichester, U.K., 1996.
- (14) Desiraju, G. R. *Angew. Chem., Int. Ed. Engl.* **1995**, *34*, 2311; See also Allen, F. H.; Hoy, V. J.; Howard, J. A. K.; Thalladi, V. R.; Desiraju, G. R.; Wilson, C. C.; McIntyre, G. J. *J. Am. Chem. Soc.* **1997**, *119*, 3477.
- (15) Aakeröy, C. B.; Beatty, A. M.; Helfrich, B. A. *Angew. Chem., Int. Ed. Engl.* **2001**, *40*, 3240.
- (16) Overgaard, J.; Schiott, B.; Larsen, F. K.; Iverson, B. B. *Chem. Eur. J.* **2001**, *7*, 3756.
- (17) Cannizzaro, C. E.; Houk, K. N. *J. Am. Chem. Soc.* **2001**, *123*, 9264.
- (18) Raymo, F. M.; Bartberger, M. D.; Houk, K. N.; Stoddart, J. F. *J. Am. Chem. Soc.* **2002**, *124*, 7163.
- (19) Henry, M. *Chem. Phys. Chem.* **2002**, *3*, 561.
- (20) Bader, R. F. W. *Atoms in Molecules—A Quantum Theory*; Oxford University Press: Oxford, U.K., 1990.
- (21) Dobado, J. A.; Martinez-Garcia, H.; Molina, J.; Sundberg, M. R. *J. Am. Chem. Soc.* **1999**, *121*, 3156; **2000**, *122*, 1144.
- (22) Macchi, P.; Iverson, B. B.; Sironi, A.; Chakoumakos, B. C.; Larsen, F. K. *Angew. Chem., Int. Ed.* **2000**, *39*, 2719.
- (23) Malcolm, N. O. J.; Popelier, P. L. A. *J. Phys. Chem. A* **2001**, *105*, 7638.
- (24) Messerschmidt, M.; Wagner, A.; Wong, M. W.; Luger, P. *J. Am. Chem. Soc.* **2002**, *124*, 732.
- (25) Zhurova, E. A.; Tsirelson, V. G.; Stash, A. I.; Pinkerton, A. A. *J. Am. Chem. Soc.* **2002**, *124*, 4574.
- (26) Ghanty, T. K.; Ghosh, S. K. *J. Phys. Chem. A* **2002**, *106*, 11815.
- (27) Morokuma, K. *Acc. Chem. Res.* **1977**, *10*, 294.

- (28) Chen, W.; Gordon, M. S. *J. Phys. Chem.* **1996**, *100*, 14316.
- (29) (a) Becke, A. D. *J. Chem. Phys.* **1993**, *98*, 1372, 5648. (b) Lee, C.; Yang, W.; Parr, R. G. *Phys. Rev. B* **1988**, *37*, 785.
- (30) Schmidt, M. W.; BalDridge, K. K.; Boatz, J. A.; Elbert, S. T.; Gordon, M. S.; Jensen, J. H.; Koseki, S.; Matsunaga, N.; Nguyen, K. A.; Su, S. J.; Windus, T. L.; Dupuis, M.; Montgomery, J. A., Jr. *J. Comput. Chem.* **1993**, *14*, 1347.
- (31) Tomasi, J.; Persico, M. *Chem. Rev.* **1994**, *94*, 2027; Cammi, R.; Tomasi, J. *J. Comput. Chem.* **1995**, *16*, 1449.
- (32) Klieger-Konig, F. W.; Bader, R. F. W.; Tang, T. H. *J. Comput. Chem.* **1982**, *3*, 317.
- (33) Guerra, C. F.; Bickelhaupt, F. M.; Snijders, J. G.; Baerends, E. J. *Chem. Eur. J.* **1999**, *5*, 3581.
- (34) Guerra, C. F.; Bickelhaupt, F. M.; Baerends, E. J. *Cryst. Growth Des.* **2002**, *2*, 239.
- (35) Guerra, C. F.; Bickelhaupt, F. M.; Snijders, J. G.; Baerends, E. J. *J. Am. Chem. Soc.* **2000**, *122*, 4117.
- (36) Shishkin, O. V.; Sponer, J.; Hobza, P. *J. Mol. Struct.* **1999**, *477*, 15.
- (37) Steiner, T.; Majerz, I.; Wilson, C. C. *Angew. Chem., Int. Ed.* **2001**, *40*, 2651.
- (38) Steiner, T.; Saenger, W. *Acta Crystallogr. B* **1994**, *50*, 348.